Catalytic-rate improvement of a thermostable malate dehydrogenase by a subtle alteration in cofactor binding

Richard M. ALLDREAD,* David M. HALSALL,† Anthony R. CLARKE,† Trichur K. SUNDARAM,‡ Tony ATKINSON,* Michael D. SCAWEN*§ and David J. NICHOLLS*

*Division of Biotechnology, Centre for Applied Microbiology and Research, Porton, Salisbury SP4 0JG, Wilts., †Molecular Recognition Centre and Department of Biochemistry, University of Bristol, Bristol BS8 1TD, and ‡Department of Biochemistry, University of Manchester Institute of Science and Technology, Manchester M60 1QD, U.K.

The nucleotide-binding fold of many NAD^+-dependent dehydrogenases contains a conserved acidic amino acid residue which hydrogen-bonds with the 2′- and 3′-hydroxy groups of the adenine-ribose of the cofactor. This residue is highly conserved as aspartate in malate dehydrogenases, except in the thermophilic enzyme from *Thermus aquaticus* B (*Taq*MDH), which has glutamic acid-41 in the equivalent position. The catalytic mechanism was dissected to investigate the functional significance of this difference in *Taq*MDH with respect to a mutant enzyme where glutamic acid-41 was replaced by aspartic acid. The mutant enzyme was found to retain a high degree of protein structural stability to both thermal and chemical denaturation. When compared with the wild-type enzyme the mutant had a higher K_m and K_d for both reduced and oxidized cofactors (NADH and NAD^+) and a 2–3-fold increase in steady-state $k_{cat.}$ in both assay directions. The rate-determining step for the reduction of oxaloacetate by wild-type *Taq*MDH was shown to be the rate of NAD^+ release, which was about 2.5-fold higher for the mutant enzyme. This correlates well with the 1.8-fold higher steady-state $k_{cat.}$ of the mutant enzyme and represents an improvement in the steady-state $k_{cat.}$ of a thermophilic enzyme at moderate temperature by a conservative amino acid substitution which increases the rate of product release.

INTRODUCTION

Thermus spp. are thermophilic prokaryotes with an optimum growth temperature of 70–80 °C and provide a good source of enzymes with high intrinsic thermal and chemical stability. Robust enzyme catalysts have applications in chemical conversions that require a high degree of specificity and operational stability. When used as diagnostic reagents the most desirable enzymes are also required to have high catalytic activity at moderate temperatures. Despite the advantage of enhanced stability, a common problem which precludes the use of thermophilic enzymes in many commercial applications is that they are generally less active at moderate temperatures than their mesophilic counterparts.

Malate dehydrogenase (MDH) catalyses the interconversion of oxaloacetate and malate linked to the oxidation or reduction of dinucleotide cofactors. This reaction is important in cellular metabolism and, as it is coupled with easily detectable cofactor oxidation/reduction, MDH has found many applications as a diagnostic linker enzyme to identify various metabolites and enzyme activities (MacGregor and Matschinsky, 1984; Wraight et al., 1985). MDH is also a good model to investigate the potential for the improvement of an enzyme by design, as it is widely distributed in both mesophilic and thermophilic organisms, and X-ray-crystallographic structures have been solved for pig heart mitochondrial MDH (Roderick and Banaszak, 1986), pig heart cytosolic MDH (Birktoft et al., 1989), *Escherichia coli* MDH (Hall et al., 1992) and *Thermus flavus* MDH (Kelly et al., 1993). MDHs are multimeric enzymes consisting of identical subunits, usually organized as either dimers or tetramers with subunit molecular masses of 30–35 kDa (Banaszak and Bradshaw, 1975; Sundaram et al., 1980). Comparisons of structural and amino-acid-sequence data have identified a number of functionally important residues which are conserved in all the MDHs. Each subunit of MDH contains a dinucleotide-binding domain which is similar in sequence and structure to that of other nicotinamide-nucleotide-dependent enzymes (Birktoft and Banaszak, 1984). X-ray structures of MDH show the bound cofactor to be in an extended conformation (Hill et al., 1972; Birktoft et al., 1989) and similar to the conformation of cofactor bound to lactate dehydrogenase (LDH) (Piontek et al., 1990). The nicotinamide ring is located towards the centre of the subunit and adjacent to the internal cavity that accommodates the substrate. The adenine group is located in a hydrophobic pocket with the adenine-ribose bound to the enzyme primarily by hydrogen-bonding and hydrophobic interactions (Birktoft and Banaszak, 1984).

*Taq*MDH is an α_2 dimer with a subunit molecular mass of 35.4 kDa and is highly stable to thermal and chemical denaturation (Sundaram et al., 1980; Smith et al., 1982). We have previously cloned the MDH gene, *mdh*, from *T. aquaticus* B in *E. coli* and determined its nucleotide sequence (Nicholls et al., 1990). Expression of the *Taq*MDH from the recombinant clone in *E. coli* was initially at a level of about 0.1 % of the soluble cell protein. This was enhanced to about 50 % by genetic manipulation of the transcription and translation initiation signals (Alldread et al., 1992). The amino acid sequence of *Taq*MDH predicted from the gene sequence was identical with that of *T. flavus* MDH and had 53 % amino acid sequence identity with porcine cytosolic MDH; for the last two enzymes there are high-

Abbreviations used: MDH, malate dehydrogenase; *Taq*MDH, *Thermus aquaticus* B malate dehydrogenase; LDH, lactate dehydrogenase; GdmCl, guanidinium chloride; *mdh*, malate dehydrogenase gene.

§ To whom correspondence should be addressed.

resolution X-ray structures (Birktoft et al., 1989; Kelly et al., 1993). The residues identified as being important for substrate binding and catalysis in mesophilic MDHs are well conserved in *Taq*MDH. One notable difference is glutamic acid-41, which is conserved as aspartic acid-41 in all other NAD^+-dependent MDHs and in the closely related LDHs. The X-ray structures of pig heart cytosolic MDH and *E. coli* MDH show that aspartic acid-41 forms hydrogen-bonding interactions with the 2′- and 3′-hydroxy groups of the adenine-ribose of the cofactor (Birktoft et al., 1989; Hall et al., 1992). In the NAD^+-specific enzymes this acidic residue is conserved at the end of the characteristic fingerprint region which defines the nucleotide-binding fold. This acidic residue is not found in $NADP^+$-specific dehydrogenases, and the importance of this region has been illustrated by engineering amino acid substitutions which modify the relative $NAD^+/NADP^+$ specificity of MDH (Nishiyama et al., 1993), LDH (Feeney et al., 1990), pyruvate dehydrogenase (Bocanegra et al., 1993), dihydropteridine reductase (Grimshaw et al., 1992), *S*-adenosylhomocysteinase (Gomi et al., 1990), alcohol dehydrogenase (Chen et al., 1991), glutathione reductase (Mittl et al., 1993) and glyceraldehyde-3-phosphate dehydrogenase (Clermont et al., 1993).

We report here a detailed examination of the catalytic step of *Taq*MDH and show how the conservative amino acid replacement of glutamic acid-41 with aspartic acid enhances the catalytic rate of this thermophilic enzyme at moderate temperatures without affecting the cofactor specificity.

MATERIALS AND METHODS

Materials

Chemicals were purchased from either BDH Chemicals Ltd. (Poole, Dorset, U.K.) or Sigma Chemical Co. (Poole, Dorset, U.K.) and were of the highest grade available. The following were 'Ultra pure' grade and supplied by BRL/GIBCO (Paisley, Renfrewshire, Scotland, U.K.): urea, CsCl, agarose, ammonium persulphate and phenol. Radiolabelled compounds were obtained from Amersham International (Amersham, Bucks., U.K.), and components of microbial growth media from Difco Laboratories (West Molesey, Surrey, U.K.). Protein molecular-mass markers and consumables for the PhastGel system were supplied by Pharmacia Ltd. (Milton Keynes, U.K.). NAD^2H was prepared as described previously (Oppenheimer et al., 1971).

Bacterial strains, plasmids and phage vectors

The host strains for recombinant plasmids and phage were: *E. coli* TG1 [*Sup*E, *hsd* 5, *thi*, (*lac-pro*AB), (F′, *tra*D36, *pro*AB^+, *lacI*^{q}, *lacZ*, M15)] and *E. coli* BMH71-18 *mut*L [(*lac*, *pro*), *thi*, (F′, *pro*AB^+, *lac*I, *lac*Z, M15), *sup*E, *mut*L::Tn10]. The pMTL series plasmids and phages used in the present study have been described by Chambers et al. (1988). The recombinant plasmids pRMA41 and pRMA51 used for production of *Taq*MDH are described by Alldread et al. (1992). *E. coli* strains were routinely grown aerobically at 37 °C in YT broth (2% tryptone/ 2% yeast extract/1% NaCl, pH 7.4). Solid plate medium was prepared by addition of agar to 2% (w/v) and supplemented with ampicillin to 100 μg/ml when required. Bacteriophage M13 was propagated in the appropriate *E. coli* host strain in YT broth.

DNA manipulations

Standard recombinant DNA techniques were performed as described by Sambrook et al. (1989).

Oligodeoxyribonucleotides for use as sequencing primers and in site-directed mutagenesis were synthesized using an Applied Biosystems model 380A DNA synthesizer. Site-directed mutagenesis to produce the glutamic acid-41→aspartic acid change was performed on single-stranded recombinant M13 template DNA by the primer-extension method as described by Carter et al., (1985), using the oligonucleotide 5′-ACCTTTTGGAC-ATCCCCCAGG-3′. An *Eco*RI–*Aat*II DNA fragment containing the mutation was used to replace a similar fragment from pRMA41 carrying the wild-type (*Taq*) *mdh* gene. The entire mutant gene was then introduced into the high-expression vector pMTL1003 as an *Nde*I–*Pst*I fragment. The resulting construct contained the mutated *Taq mdh* gene and had a similar structure to the high-expression plasmid pRMA51 described previously for the wild-type *Taq mdh* gene (Alldread et al., 1992). The presence of the mutation and the absence of spurious mutations were confirmed by nucleotide sequencing, using the chain-termination procedure (Sanger et al., 1977) and Sequenase (United States Biochemicals Corp.) and 7-deoxydeazaguanosine triphosphate (BCL, Lewes, East Sussex, U.K.) to diminish sequencing compressions in the G/C rich *Thermus*-derived DNA.

Enzyme activity and protein assays

MDH activity was measured by determining the change in absorbance at 340 nm due to NADH oxidation or reduction. One unit of activity is defined as that catalysing the oxidation of 1 μmol of NADH/min at 30 °C in 60 mM sodium phosphate buffer, pH 7.5, containing 0.14 mM NADH and 0.3 mM oxaloacetate. Steady-state kinetics were determined at temperatures between 30 and 60 °C in 60 mM sodium phosphate buffer, pH 7.5, with constant substrate concentrations of 0.14 mM NADH, 0.3 mM oxaloacetate, 10 mM NAD^+ and 10 mM malate. (Note: it was not conveniently possible to make measurements above 60 °C because of the instability of the substrates, NADH and oxaloacetate, at elevated temperatures.) Steady-state parameters were calculated by non-linear regression analysis of the data (Enzfitter; Biosoft, Cambridge, U.K.). The protein concentration in cell extracts was determined by the biuret method (Gornall et al., 1949). For purified *Taq*MDH preparations, the protein concentration was determined by using the relationship $A_{280}^{1\%} = 9.0$ calculated from amino-acid-composition data.

Protein purification and gel electrophoresis

Wild-type and mutant enzymes were purified largely as described by Aldread et al. (1992). Cells were harvested from 10 litre cultures of *E. coli* containing the plasmid expressing either the wild-type or mutant *Taq*MDH. A cell extract (150 ml) was made and heated at 80 °C for 30 min. The precipitate of *E. coli* proteins was removed by centrifugation and the supernatant diluted to 1 litre with distilled water. This was loaded on to a 100 ml (bed volume) column of Procion Red HE-3B linked to Sepharose. The column was washed with (i) 200 ml of 10 mM sodium phosphate buffer, pH 7.2, (ii) 200 ml of phosphate buffer containing 10 mM KCl, (iii) 100 ml of phosphate buffer, (iv) 50 ml of phosphate buffer containing 10 mM L-malate, (v) 50 ml of phosphate buffer, (vi) 100 ml of phosphate buffer containing 0.4 mM NAD^+, and (vii) 100 ml of phosphate buffer. *Taq*MDH was eluted from the column with phosphate buffer containing 10 mM malate and 0.4 mM NAD^+. The active fractions were pooled and stored at 4 °C as a precipitate in 85%-satd. $(NH_4)_2SO_4$. PAGE was performed using the PhastGel system (Pharmacia).

Rapid-reaction spectroscopy

Rapid-reaction enzyme kinetic studies were carried out using a Hi-Tec SF-51 stopped-flow spectrophotometer (Hi-Tec Scientific Instruments Ltd., Salisbury, Wilts., U.K.) at 30 °C. For single-turnover experiments, 115 μM enzyme and 80 μM NADH were rapidly mixed with 1mM oxaloacetate and the reaction monitored by the change in absorbance at 340 nm. For multiple-turnover experiments, 115 μM enzyme and 500 μM NADH were rapidly mixed with 1 mM oxaloacetate and the reaction monitored by the change in absorbance at 340 nm. Rate constants were determined by non-linear regression analysis of the single-exponential transients using the software supplied by the instrument manufacturer. The data were corrected for the dead time of the apparatus, which was calculated independently. Transient rate experiments to determine kinetic constants were carried out at 30 °C, rather than 60 or 70 °C, because the rates of reaction at the higher temperatures were beyond the limits of detection of the stopped-flow spectrophotometer.

The rate of NAD^+ dissociation was determined at 30 °C by premixing 115 μM enzyme and 115 μM NAD^+ to form the enzyme–NAD^+ binary complex. This was rapidly mixed with 2.3 mM NADH to displace the equilibrium in favour of the enzyme–NADH binary complex. The rate of formation of this complex was monitored by the increase in fluorescence emission at 453 nm (with excitation at 340 nm). As the binding of NADH is a diffusion-controlled reaction, it is rapid at high concentrations of NADH, and the apparent rate of formation of the enzyme–NADH complex is a good approximation of the much lower NAD^+ dissociation rate.

Determination of protein thermal stability

The thermal stability of *Taq*MDH was measured for irreversible enzyme inactivation at 97 °C. The enzyme was incubated at a concentration of 100 μg/ml in 20 mM sodium phosphate buffer, pH 7.2. Phosphate buffer was used as there is only a small change in its pH with temperature. Aliquots (50 μl) of the enzyme sample were placed in 0.5 ml glass tubes and incubated at 97 °C for various time periods. After incubation, all tubes were placed on ice for a relaxation time of 20 min before assay for residual activity. A single tube left on ice for the duration of the experiment was used as the zero-time control.

Dependence of enzyme activity on pH

Steady-state enzyme assays were performed for both wild-type and mutant enzymes using three overlapping buffer systems in the range pH 5.5–10.0. The buffers used were all at a concentration of 100 mM: Mops, pH 5.5–7.5; Hepes, pH 7.0–9.0; and Tris/HCl, pH 8.0–10.0; each buffer contained 200 mM NaCl to ensure a high and constant ionic strength. Solutions were adjusted to the correct pH with 100 mM HCl or NaOH as required. Concentrations of substrates were the same as for the standard assays.

Equilibrium unfolding in guanidinium chloride (GdmCl)

An initial scan of emission wavelengths with an excitation wavelength of 295 nm showed that the emission maximum for each enzyme was 329 nm. A preliminary study showed that an incubation time of 16 h in GdmCl was required to ensure that an unfolding equilibrium had been reached. Unfolding in GdmCl was established to be a reversible process, as fully active enzyme was recovered after the enzyme was incubated in 5 M denaturant and then diluted 1000-fold in sodium phosphate buffer. Wild-type and mutant enzymes at 100 μg/ml were incubated in 50 mM sodium phosphate buffer, pH 7.4, with 1 mM dithiothreitol and various concentrations of GdmCl from 0 to 5 M. The change in fluorescence emission at 329 nm was monitored using a Perkin–Elmer LS5 fluorescence spectrophotometer. Data were corrected for the emission of a buffer blank containing dithiothreitol. The conformational free energy in the absence of denaturant ($\triangle G_{H_2O}$) and the midpoint of the unfolding were calculated by non-linear regression analysis of the corrected data (Pace, 1986, 1990).

Determination of NADH dissociation constant

The enhancement in NADH fluorescence emission on the formation of the enzyme–NADH binary complex was used to determine K_d for NADH. A 200 μM solution of enzyme was added to 3 ml of a 5 μM NADH solution in 5–10 μl aliquots. The fluorescence was measured with excitation at 340 nm and emission at 453 nm using a Perkin–Elmer LS5 fluorescence spectrophotometer at room temperature (20–22 °C). The fluorescence data and enzyme concentrations were corrected for dilution and the dissociation constant calculated by non-linear regression analysis using a binding equation which assumes that the concentration of bound ligand is significant compared with free ligand:

$$F = \{(K+E+L) - \sqrt{[(K+E+L)^2 - 4EL]}\}/2E \cdot (F_x - F_n) + F_n$$

Where F is the observed fluorescence, K is the dissociation constant (K_d), E is the concentration of enzyme, L is the concentration of ligand (NADH), S_x the fluorescence of bound NADH and S_n the fluorescence of free NADH.

Determination of NAD^+ dissociation constant

The K_d for NAD^+ was determined at 30 °C by monitoring the decrease in enzyme fluorescence of the enzyme–NAD^+ binary complex compared with the higher fluorescence of free enzyme in solution. An emission scan of the enzyme with and without 100 μM NAD^+ at an excitation wavelength of 295 nm showed that the maximum fluorescence difference due to NAD^+ binding occurred at an emission wavelength of 330 nm. The fluorescence was monitored as a 1 mM solution of NAD^+ was added in 10 μl aliquots to a 10 μM enzyme solution. The fluorescence readings were corrected for the inner-filter effect of NAD^+ by monitoring the fluorescence emission of *N*-acetyltryptophanamide as a control. NAD^+ concentrations were corrected for dilution, and the dissociation constant was calculated by non-linear regression fitting to a simple ligand-binding equation which assumes one binding site for NAD^+ per subunit of enzyme. The measurements were carried out at room temperature (20–22 °C).

RESULTS

Mutagenesis of the *Taq mdh* gene, its expression and purification of the mutant enzyme

The mutated *Taq mdh* gene containing the directed change glutamic acid-41→aspartic acid was incorporated into the plasmid vector pMTL1003 for overexpression in *E. coli*. The mutant *Taq*MDH was produced at a level that represented about 50% of the soluble cell protein, which is comparable with the level of expression of the wild-type *Taq*MDH in *E. coli*. Purifications of both mutant and wild-type enzymes were performed in the same way by Procion Red HE-3B triazinyl-dye affinity chromatography. As triazinyl dyes interact with nucleotide-binding sites in proteins (Biellmann et al., 1993) it was possible that the mutation glutamic acid-41→aspartic acid, at the nucleotide-binding site could adversely affect the purification procedure for the mutant enzyme. However, the affinity of immobilized Procion Red HE-

Table 1 Purification of wild-type and mutant *Taq*MDH

Purifications were performed using Procion Red HE-3B dye affinity chromatography as described in the Materials and methods section.

Enzyme preparation	Total activity (units)	Total protein (mg)	Specific activity (units/mg)	Recovery (%)
Wild-type				
Cell extract	64000	670	96	100
Heated cell extract	64000	382	168	100
Eluted enzyme	26000	133	195	41
Mutant				
Cell extract	78000	460	170	100
Heated cell extract	78000	262	298	100
Eluted enzyme	46500	122	380	60

Table 2 Thermal and chemical stability of wild-type and mutant *Taq*MDH

Irreversible thermal inactivation at 97 °C and unfolding in GdmCl were determined as described in the Materials and methods section. Standard errors were given by the curve-fitting program Enzfitter.

	Thermal stability ($t_{\frac{1}{2}}$)		GdmCl stability	
Enzyme	−NADH	+NADH	Unfolding midpoint (M)	Unfolding energy ΔG_{H_2O} (kJ·mol^{-1})
Wild-type	17.2±2.9	24.5±4.6	2.98±0.28	24.5±1.2
Mutant	17.7±3.2	19.7±3.5	3.04±0.39	24.2±1.6

Table 3 Steady-state catalytic constants and K_d values for wild-type and mutant *Taq*MDHs at 30 °C

Standard errors were given by the curve-fitting program Enzfitter. Abbreviation: ND, not determined.

Enzyme	Parameter	Substrate or cofactor ...	Oxaloacetate	Malate	NADH	NAD^+	NADPH
Wild-type	K_d (μM)		ND	ND	9.5±0.15	20.0±2.3	ND
	K_m (μM)		14.0±1.5	41.0±6.8	8.1±0.8	21.0±3.6	190.0±7.1
	$k_{cat.}$ (s^{-1})		144±4.8	3.2±0.14	146.0±3.4	2.3±0.1	37.0±0.8
	$k_{cat.}/K_m$ ($mM^{-1}\cdot s^{-1}$)		10300±1450	78±16	18000±2200	110±24	195±12
Mutant	K_d (μM)		ND	ND	16.0±0.6	200±14	ND
	K_m (μM)		15.0±1.6	52.0±7.6	16.0±1.3	68.0±6.4	230±14
	$k_{cat.}$ (s^{-1})		264±9	7.7±0.3	283±7	6.1±0.2	44.0±2.2
	$k_{cat.}/K_m$ ($mM^{-1}\cdot s^{-1}$)		17600±2500	150±28	17700±1880	90±11	190±21

3B for the mutant enzyme was apparently similar to that for the wild-type enzyme (Table 1). The final preparations of the wild-type and mutant enzymes were over 95% homogeneous as judged by SDS/PAGE gels stained with Coomassie Blue. The most notable difference between the purifications was in specific activity: the purified mutant enzyme (380 units/mg) was nearly 2-fold higher than that of the purified wild-type enzyme (195 units/mg) (Table 1).

Thermal and chemical stability

Thermal-stability data for the wild-type and mutant *Taq*MDHs at 97 °C in the absence and presence of NADH are shown in Table 2. The thermal stability of the apoenzyme was very similar for both wild-type and mutant enzymes, and the presence of NADH appeared to have a small stabilizing effect on both enzyme forms. The effect was rather greater on the wild-type enzyme, where the half-life of the apoenzyme at 97 °C was increased by 7.3 min in the presence of NADH compared with an increase of only 2 min for the mutant enzyme.

The chemical denaturant GdmCl facilitates protein unfolding by increasing the solubility of apolar amino acid side chains in water. Fluorescence spectroscopy was used to measure the extent of protein denaturation on the basis that the fluorescence intensity of tryptophan side chains buried in the native enzyme is diminished by solvent quenching as the protein unfolds. Both wild-type and mutant enzymes produced a simple two-state unfolding transition occurring between 2.5 and 3.5 M GdmCl. The midpoint for unfolding and ΔG_{H_2O} were similar for both enzymes (Table 2).

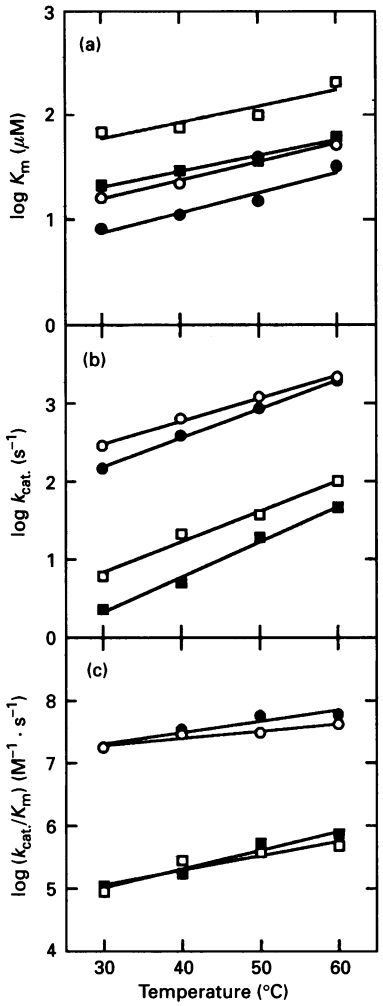

Figure 1 Effect of temperature on cofactor steady-state constants

The steady-state constants (**a**, K_m; **b**, $k_{cat.}$; **c**, $k_{cat.}/K_m$) for NADH and NAD^+ were determined as described in Materials and methods section. Determinations were made for the wild-type and mutant enzymes at various temperatures as indicated. Wild-type enzyme and NADH (●), wild-type enzyme and NAD^+ (■), mutant enzyme and NADH (○), mutant enzyme and NAD^+ (□).

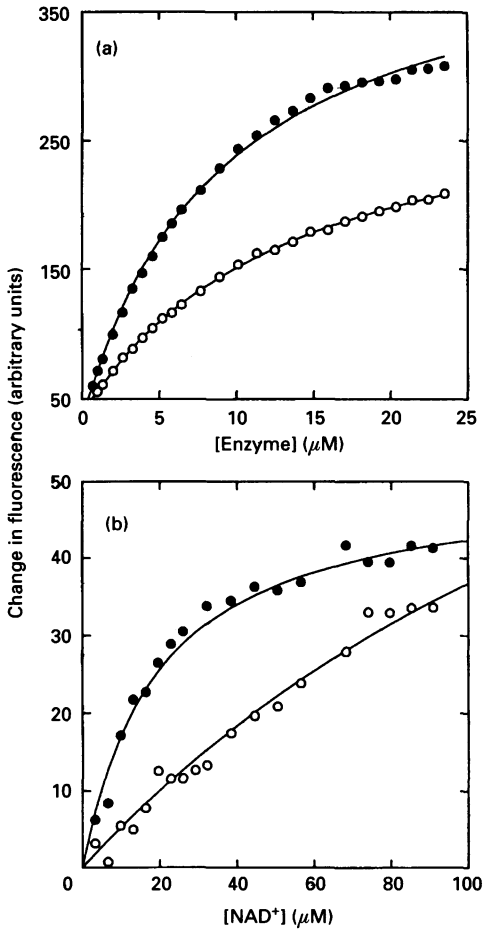

Figure 2 Determination of cofactor dissociation constants

(**a**) The fluorescence of NADH was measured over a range of increasing enzyme concentrations. (**b**) The effect of NAD^+ binding on protein fluorescence was determined at a range of cofactor concentrations. ●, Wild-type enzyme; ○, mutant enzyme.

Steady-state catalysis parameters

For the reduction of oxaloacetate both the wild-type and mutant enzymes had a similar pH optimum of about pH 9.0, suggesting that there was no significant alteration in the ionization characteristics of enzyme catalysis as a result of the mutation. Steady-state kinetic constants and cofactor binding constants for both wild-type and mutant enzymes determined at 30 °C are presented in Table 3. There were no significant differences between the wild-type and mutant enzymes in the values of K_m for oxaloacetate and malate. The main differences between the two enzyme forms were in the steady-state $k_{cat.}$ values obtained for both substrates and cofactors. Values of steady state $k_{cat.}$ for the mutant enzyme were nearly 1.8-fold higher than for the wild-type enzyme in the direction of oxaloacetate reduction, with a parallel and similar increase of nearly 2-fold in the K_m for NADH (Table 3). In the direction of malate oxidation the mutant enzyme showed an increase in $k_{cat.}$ of 2–3-fold and a parallel increase of about 3-fold in K_m for NAD^+, compared with the wild-type enzyme. The effect of the mutation on catalytic efficiency at 30 °C (as measured by $k_{cat.}/K_m$) was marginal with respect to both cofactors, as the enhancement in $k_{cat.}$ was compensated for by an increase of similar magnitude in cofactor K_m (Table 3). However, as there was no change in the substrate K_m, an apparent 2-fold increase in catalytic efficiency was observed for the mutant enzyme.

Effect of temperature on steady-state catalysis

The effect of assay temperature on the steady-state constants for both cofactors determined with the wild-type and mutant enzymes is shown in Figure 1. The values of K_m and $k_{cat.}$ for the cofactors increased with temperature in a roughly parallel fashion (Figures 1a and 1b). Similarly, the catalytic efficiency ($k_{cat.}/K_m$) for both enzymes with respect to the cofactors increased with temperature. It appears that the differences in $k_{cat.}$ and K_m between the two enzymes are maintained at higher temperatures and consequently no significant difference in catalytic efficiency between them was seen as the temperature was raised (Figure 1c).

From the standpoint of catalytic efficiency the wild-type and mutant enzymes both showed a considerable preference for NADH over NADPH at 30 °C (Table 3). At 60 °C the K_m for NADPH for both enzymes was too high to be conveniently

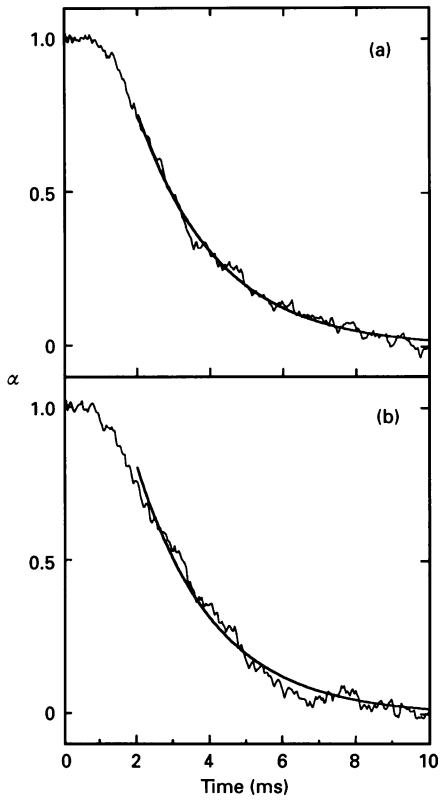

Figure 3 Single-turnover catalytic rates

A solution of 115 μM enzyme and 80 μM NADH was rapidly mixed with 1 mM oxaloacetate and the absorbance measured at 340 nm. The results are presented as the fractional change in absorbance α, defined as $(A_0 - A_f)/(A_i - A_f)$, where A_f is the final absorbance, A_i is the initial absorbance and A_0 is the observed absorbance measured with time. (**a**) Wild-type enzyme; (**b**) mutant enzyme. The thin wavy line represents the experimental data; the (bolder) curve shows the single-exponential-decay fit.

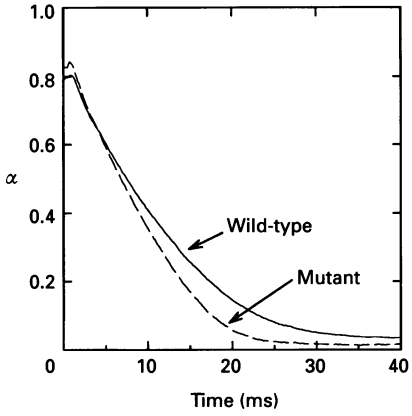

Figure 4 Multiple-turnover catalytic rates

A solution of 115 μM enzyme and 500 μM NADH was rapidly mixed with 1 mM oxaloacetate, and the change in absorbance was measured at 340 nm. The results are presented as the fractional change in absorbance, α (defined in the legend to Figure 3). The continuous line shows the results for the wild-type enzyme and the broken line shows those for the mutant enzyme; the broken line indicates the contribution to the reaction of the initial single turnover after 25% of the NADH has been used.

measured. However, estimates of $k_{cat.}/K_m$ obtained from linear plots of rate versus NADPH concentration (results not shown) were similar for both wild-type and mutant enzymes at 40 and 39 $mM^{-1} \cdot s^{-1}$ respectively This represents a decrease in catalytic efficiency with NADPH of about 5-fold at 60 °C compared with the efficiency at 30 °C and is in marked contrast with the enhanced catalytic efficiency observed with NADH at elevated temperatures (Figure 1c).

Cofactor binding affinity

The dissociation constants for NADH were determined at 30 °C from the enhancement in fluorescence emission of the enzyme–NADH binary complex as compared with free NADH in solution (Figure 2a). The mutation weakened the NADH binding affinity of the enzyme, as shown by an increase in K_d of about 2-fold for the mutant enzyme compared with the wild-type enzyme (Table 3). These values agree closely with the K_m values for the wild-type and mutant enzymes. The dissociation constants for NAD^+ were also determined at 30 °C by fluorescence spectroscopy. As NAD^+ is not fluorescent, the enhancement in tryptophan fluorescence that occurs when enzyme binds NAD^+ to form the enzyme–NAD^+ binary complex was monitored (Figure 2b). The K_d for NAD^+ was 10-fold higher for the mutant than for the wild-type enzyme (Table 3), demonstrating that the mutation glutamic acid-41→aspartic acid had considerably weakened the binding affinity for NAD^+.

Single-turnover catalytic rates

Enzyme and NADH were premixed in equimolar concentrations sufficiently high to ensure formation of the binary complex, and the rate of reaction was monitored under psuedo-first-order conditions in a stopped-flow spectrophotometer (Figure 3). In these experiments it was important that the concentration of NADH should not exceed the concentration of enzyme to ensure that only a single turnover occurred. The wild-type and mutant enzymes had similar single turnover rates of 431 and 413 s^{-1}, which were considerably higher than the respective steady-state $k_{cat.}$ values of 146 and 283 s^{-1} (Table 3). To determine whether hydride transfer was rate-limiting, the single-turnover stopped-flow experiment was repeated with the wild-type enzyme using NAD^2H. As the deuteride ion of NAD^2H is transferred to the substrate more slowly than the hydride of NADH, a mechanism that was rate-limited by hydride transfer would show a decrease in catalytic rate with NAD^2H. Typically, for this type of mechanism the ratio $k(NADH)/k(NAD^2H)$ would be expected to be between 3 and 6 (Lodola et al., 1978). For the wild-type MDH the single turnover rate obtained with NAD^2H was 373 s^{-1}, giving a $k(NADH)/k(NAD^2H)$ ratio of 1.16, indicating that hydride transfer is not rate-limiting. The mutant enzyme would also not be limited by hydride transfer as the single-turnover rates of the wild-type and mutant enzymes were similar.

Multiple-turnover catalytic rates

A multiple-turnover experiment was performed to provide a qualitative indication as to whether the rate-determining step in steady-state catalysis occurs after the catalytic step. Rapid-mixing experiments were done with a 4-fold molar excess of NADH over the enzyme (Figure 4). The starting point of the reaction was recorded with enzyme and NADH in the mixing

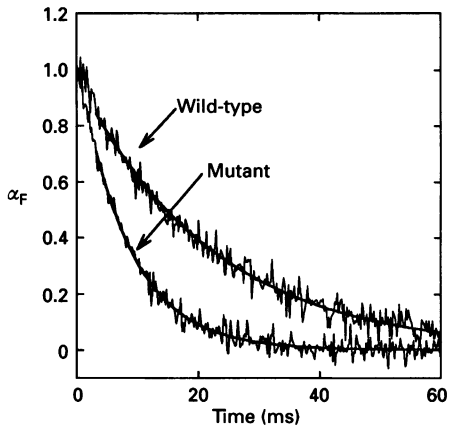

Figure 5 Rate of NAD^+ dissociation

The enzyme–NAD^+ binary complex at 230 μM was rapidly mixed with 2.3 mM NADH and the enhancement in fluorescence emission at 453 nm due to formation of the enzyme–NADH binary complex was measured (excitation wavelength 340 nm). The results are presented as the fractional change in fluorescence α_F, defined as $(F_0 - F_i)/(F_i - F_f)$, where F_f is the final fluorescence, F_i is the initial fluorescence and F_0 is the observed fluorescence measured with time. The thin wavy lines represent the experimental data and the (bolder) curves represent the single-exponential-decay fits.

chamber and the end point with the mixture of enzyme, NADH and oxaloacetate that had fully reacted. The fractional change in absorbance at 340 nm determined for both enzymes shows a rapid burst for the first catalytic turnover, with a rate of around 400 s^{-1} (Figure 4). In the subsequent turnover cycles the rate was clearly lower for both the wild-type and mutant enzymes (Figure 4). This indicates that the rate-determining step in the steady-state reaction is not the chemical conversion step but recycling of the enzyme. The multiple-turnover experiment also showed that catalytic turnovers after the initial burst were faster for the mutant enzyme (about 160 s^{-1}) than for the wild-type enzyme (about 125 s^{-1}).

NADH binding rate

The rates of NADH binding to the two enzymes were determined in the stopped-flow spectrophotometer by monitoring the enhancement in fluorescence of NADH in the enzyme–NADH binary complex. Relatively low concentrations of NADH and enzyme were required to produce transients that were slow enough to be accurately recorded. At a fixed NADH concentration (1 μM), the rate of the exponential fluorescence transient was directly proportional to the enzyme concentration in the range 2–10 μM. A plot of observed rate against enzyme concentration was linear, with a gradient equal to the second-order bimolecular rate constant (NADH on-rate). The NADH on-rates had values of 3.9×10^7 $M^{-1} \cdot s^{-1}$ for the wild-type and 3.2×10^7 $M^{-1} \cdot s^{-1}$ for the mutant enzymes, which is consistent with a diffusion-controlled reaction. The intercept of the plot, which corresponds to the NADH off-rate, was not defined (results not shown).

NAD^+ dissociation rate

Results from the single-turnover, multiple-turnover, deuterium-isotope-effect and NADH-binding-rate experiments taken together suggested that the rate-determining step was after the catalytic step. Therefore the dissociation rate of the enzyme–NAD^+ binary complex (NAD^+ off-rate) was measured, as this is the last step in the reaction. A solution of enzyme–NAD^+ binary complex was mixed rapidly with a 10-fold excess of NADH to displace the equilibrium in favour of the enzyme–NADH binary complex. As NADH binding is diffusion-controlled, it is rapid at high concentrations, and the apparent rate of formation of the enzyme–NADH binary complex provides a good approximation of the much lower NAD^+ off-rate. This represented the lowest observed rate in the reaction mechanism at 45.5 s^{-1} for the wild-type and 114 s^{-1} for the mutant enzymes respectively (Figure 5). There was a strong correlation between the degree of enhancement in the NAD^+ off-rate and the increase in steady-state $k_{cat.}$ found for the mutant enzyme, which was about 2–3-fold in both cases.

Effect of solvent viscosity

The question of whether the release of NAD^+ involves a conformational change in the enzyme was investigated on the basis that the rates of protein conformational changes are reduced in more viscous bulk solvents (Demchenko et al., 1989). The K_m and $k_{cat.}$ values for oxaloacetate were determined in a solution of 40% glycerol at 30 °C (Table 4). For both enzyme forms there was a decrease in K_m and $k_{cat.}/K_m$ due to the lower dielectric constant of 40% glycerol, which increases the magnitude of electrostatic interactions to enhance substrate binding affinity. For both enzymes the steady-state $k_{cat.}$ was reduced in the presence of glycerol, indicating that the rate-determining step is a protein conformational change. Such a change has been proposed previously as the rate-determining step for other dehydrogenase enzymes (Frieden and Fernandez Sousa, 1975; Whitaker et al., 1974; Clarke et al., 1985; Waldman et al., 1988). The steady-state $k_{cat.}$ was over 8-fold higher for the mutant enzyme in 40% glycerol than for the wild-type enzyme. The mutant enzyme is thus less susceptible than the wild-type enzyme to viscosity effects.

Table 4 Effect of solvent viscosity on steady-state kinetic constants for oxaloacetate

Standard errors were given by the curve-fitting program Enzfitter.

	No glycerol			40% Glycerol		
Enzyme	K_m (μM)	$k_{cat.}$ (s^{-1})	$k_{cat.}/K_m$ ($mM^{-1} \cdot s^{-1}$)	K_m (μM)	$k_{cat.}$ (s^{-1})	$k_{cat.}/K_m$ ($mM^{-1} \cdot s^{-1}$)
Wild-type	14.0±1.5	144±5	10300±1480	4.0±0.3	5.0±0.5	1300±230
Mutant	15.0±1.6	264±9	17600±2480	4.0±0.2	33.0±2.3	8300±990

DISCUSSION

Stability

In the absence of NADH the wild-type and mutant enzymes had comparable stability to thermal inactivation and chemical denaturation, suggesting that residue 41 does not contribute significantly to the structural stability of the apoenzyme. However, the thermal stabilities of both wild-type and mutant enzymes were enhanced in the presence of NADH. A similar, cofactor-induced, stability enhancement was observed in porcine heart mitochondrial MDH and porcine heart LDH, where the most important interactions were with the phosphate and nicotinamide groups of the coenzyme (Hones, 1985). The weaker stabilizing effect of NADH on the mutant enzyme can be explained by the lower binding affinity of this enzyme for NADH; there would be a greater proportion of the mutant apoenzyme than of the wild-type apoenzyme at a given concentration of NADH.

Nucleotide binding

The mutant enzyme showed an apparent improvement in catalytic efficiency ($k_{cat.}/K_m$) with both oxaloacetate and malate, owing to the increase in steady-state $k_{cat.}$. However, this is unlikely to be a direct effect on the transition-state complex as the mutation is remote from the substrate binding site, there was comparatively little change in substrate K_m, and the rapid-mixing experiments showed no change in the rate of hydride transfer. The similar catalytic efficiencies for cofactor of both the wild-type and mutant enzymes suggests that the mutation does not affect the binding energy for the cofactor in the productive transition-state complex (Fersht et al., 1985). This is consistent with the location of the mutation remote from the catalytically important residues of the active site. The differences in cofactor K_m and K_d suggest that the predominant effect of the mutation on catalysis is in cofactor binding to the binary complex. The mutation increased the magnitude of K_m and K_d more for NAD^+ than for NADH, suggesting that residue 41 makes a greater contribution to the overall binding affinity of NAD^+ than of NADH.

The crystal structures of various MDHs and LDHs show that a conserved carboxylate group makes hydrogen-bonding interactions with the hydroxy groups of the adenine-ribose (Birktoft et al., 1989; Hall et al., 1992). It is situated at the end of the β-sheet (βB) of the cofactor-binding domain and forms part of a crevice in which the adenine ring of the cofactor is located. *Taq*MDH has glutamic acid-41 in the equivalent position to the conserved aspartic acid in other NAD^+-dependent MDHs. The X-ray structure of *T. flavus* MDH shows that the peptide backbone has contracted to accommodate the larger side chain of glutamic acid-41 compared with aspartic acid-41 in porcine cytosolic MDH (Kelly et al., 1993). In both structures the hydrogen-bonding distances between the carboxylate group and the adenine-ribose 2- and 3-hydroxy groups of NAD^+ are similar. Replacement of glutamic acid-41 by aspartic acid in *Taq*MDH would be inconsistent with the backbone structure for efficient hydrogen-bonding with the cofactor, which would explain the observed increase in K_d.

Cofactor specificity

Glutamic acid-41 in *Taq*MDH is at a critical position with respect to cofactor specificity in view of its hydrogen-bonding interaction with the adenine-ribose 2-hydroxy group of NADH and the fact that in NADPH this hydroxy group is replaced by a phosphate group. The equivalent aspartic acid residue was replaced by a neutral amino acid in other NADH-specific dehydrogenases: MDH (Nishiyama et al., 1993), LDH (Feeney et al., 1990), pyruvate dehydrogenase (Bocanegra et al., 1993), dihydropteridine reductase (Grimshaw et al., 1992), *S*-adenosylhomocysteinase (Gomi et al., 1990), alcohol dehydrogenase (Chen et al., 1991) and glyceraldehyde-3-phosphate dehydrogenase (Clermont et al., 1993). Invariably the result was a modified enzyme with an enhanced preference for $NADP^+$/NADPH over NAD^+/NADH. These mutant enzymes can tolerate the proximity of the negatively charged phosphate group in $NADP^+$/NADPH through diminished steric hindrance and removal of a potentially unfavourable charge repulsion between the negatively charged phosphate group and the acidic side chain of the enzymes (Feeney et al., 1990). Although steric crowding around the extra phosphate of NADPH is reduced in the *Taq*MDH glutamic acid-41→aspartic acid mutant enzyme, the potential for charge repulsion with the phosphate group is still present. The comparable K_m values for NADPH of the mutant and wild-type enzymes (Table 3) indicate that the difference in side chain size is of minor importance. A similar effect was found for glyceraldehyde-3-phosphate dehydrogenase, where replacement of the equivalent residue, aspartic acid-32, by glutamic acid, produced no detectable effect on $NADP^+$ specificity (Clermont et al., 1993). These results are in agreement with the conclusion that charge repulsion is the major energy barrier for $NADP^+$ to serve as a cofactor for NAD^+-dependent alcohol dehydrogenase (Chen et al., 1991). For both wild-type and mutant *Taq*MDHs at 60 °C there was a decrease in catalytic efficiency ($k_{cat.}/K_m$) with NADPH of about 5-fold relative to the efficiency at 30 °C. This is in marked contrast with the enhanced catalytic efficiency observed with NADH at 60 °C and reflects an optimization of cofactor specificity at higher temperatures that is consistent with the preferred high growth temperature of *Thermus aquaticus*.

Mechanism

Kinetic studies of porcine mitochondrial and cytosolic MDHs have indicated that catalysis involves a compulsory ordered mechanism in which cofactor binds first and leaves last (Telegdi et al., 1973; Frieden and Fernandez-Sousa, 1975; Silverstein and Sulebele, 1969). This mechanism was assumed for *Taq*MDH as shown in Scheme 1. For both wild-type and mutant enzymes the single-turnover rates were closely similar and considerably greater than the values for steady-state $k_{cat.}$. This indicates that the steps from NADH binding up to and including the chemical conversion were not rate-limiting (Scheme 1). The deuterium-isotope effect with the wild-type enzyme also confirmed that chemical conversion was not the rate-determining step. The multiple-turnover experiment provided additional supportive evidence that the rate-determining step in steady-state catalysis was after the catalytic step, as the rate of catalysis following the first turnover was lower with both enzymes. The bimolecular rate constants for NADH association (NADH on-rate) for both enzymes approach the maximum rate attainable for a diffusion-limited process (approx. 10^8 $M^{-1}\cdot s^{-1}$) and are close to the value reported for porcine cytosolic MDH of 3.5×10^7 $M^{-1}\cdot s^{-1}$ (Frieden and Fernandez-Sousa, 1975). At high NADH concentrations, which saturate the steady-state reaction, the NADH on-rate is in excess of the steady-state $k_{cat.}$; therefore NADH binding can be discounted as the rate-determining step for oxaloacetate reduction (Scheme 1).

The rate of dissociation of NAD^+ from the enzyme–NAD^+ binary complex (NAD^+ off-rate) defined the rate-determining step in the MDH reaction, as it represented the lowest rate

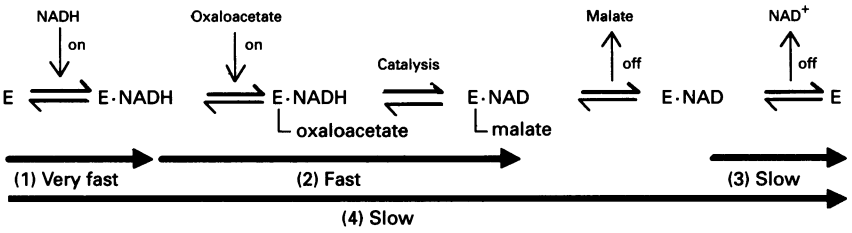

Reaction step	Relative rates (wild-type/mutant)
(1) NADH on-rate	1.2:1
(2) Single turnover rate	1:1
(3) NAD^+ off-rate	1:2.5
(4) Steady-state $k_{cat.}$	1:1.8

Scheme 1 Summary of defined steps in catalysis

Bold arrows numbered 1–4 indicate the extent and direction of each step measured. The relative rates of wild-type and mutant enzymes for each step are summarized.

measured in the stopped-flow spectrophotometer. Moreover, the NAD^+ off-rate for the mutant enzyme was approx. 2.5-fold higher than that for the wild-type enzyme, which is comparable with the 1.8-fold difference in steady-state $k_{cat.}$ between the mutant and wild-type enzymes. For both enzymes absolute values for the NAD^+ off-rates, as measured directly by stopped flow, were considerably lower than the steady-state estimates of $k_{cat.}$. The apparent paradox that a compulsory step in the reaction pathway is slightly slower than the steady-state $k_{cat.}$ has been observed before in dehydrogenases (Hart, 1989). This may be explained if the enzyme–NAD^+ binary complex in an equilibrium binding experiment is in a different conformation, which affects NAD^+ release, compared with the enzyme–NAD^+ binary complex which is continually cycling in the steady state. Of greater importance is the correlation between the increase in both steady-state $k_{cat.}$ and NAD^+ off-rate for the mutant enzyme. This increased NAD^+ off-rate is consistent with the independently observed increase in K_d for NAD^+ for the mutant enzyme ($K_d = k_{off}/k_{on}$).

Evidence for a conformational change on cofactor release

Inhibition studies on porcine mitochondrial MDH with thenoyl trifluoroacetate indicated that the enzyme existed in two different conformational forms, one of which can bind NAD^+ and the other which can bind NADH (Gutman and Hartstein, 1977). In addition, the mobility of fluorescent cofactor analogues has shown that the nicotinamide-ring-binding site of porcine mitochondrial MDH is subject to conformational changes (Hones et al., 1986a,b). Previous reports have proposed a structural rearrangement before cofactor release as the rate-determining step in porcine cytosolic MDH (Frieden and Fernandez-Sousa, 1975) and porcine heart LDH (Whitaker et al., 1974; Clarke et al., 1985). The NAD^+ on-rate for the wild-type enzyme ($2.5 \times 10^6\ s^{-1}$) calculated by using the equation $k_{on} = k_{off}/K_d$ is lower than would be expected if NAD^+ binding was a fast diffusion-limited process ($10^8\ s^{-1}$). Moreover, the reduced $k_{cat.}$ of both enzymes in glycerol implied that this rearrangement was susceptible to solvent viscosity. This is consistent with the findings for other MDHs, and the overall evidence suggests that a structural rearrangement in *Taq*MDH is associated with the release of NAD^+.

Conclusion

It appears that, in the wild-type *Taq*MDH, glutamic acid-41 is preferred over aspartic acid, as it confers a high binding affinity for cofactor at the expense of catalytic rate. This is consistent with the expected evolutionary pressures on enzyme-catalysed cellular metabolism, where the maximum turnover rate ($k_{cat.}$) at saturating cofactor concentration does not normally occur in the intracellular environment. As the rates of chemical changes are enhanced at high temperature, catalytic-rate proficiency is less critical to thermophilic enzymes than is optimization of protein stability and ligand-binding affinity. Enhanced protein stability and high ligand-binding affinity are characteristic features of thermophilic enzymes, which often persist at lower temperatures (Cowan, 1992). In wild-type *Taq*MDH the high binding affinity for NAD^+ is defined by a low off-rate, which limits the steady-state $k_{cat.}$ at moderate temperatures and is probably mediated by a structural rearrangement. Although the transient rate kinetics and cofactor-binding constants were determined at 30 °C rather than 60 °C, the essentially parallel relationship between the steady-state kinetic constants (Figure 1) suggests that the differences between the wild-type and mutant enzyme are maintained as the temperature is increased. However, all experiments were carried out at the same temperature for both enzymes, so as to provide a direct and meaningful comparison.

This work provides an example of the potential for using a stable enzyme framework for the redesign of catalytic function at lower temperatures. It shows how the introduction of mutations into thermophilic enzymes to weaken product binding may be a useful approach towards the design of custom enzymes which combine both high stability and high catalytic activity.

We thank Mr. K. Fantom for oligonucleotide synthesis.

REFERENCES

Alldread, R. M., Nicholls, D. J., Sundaram, T. K., Scawen, M. D. and Atkinson, T. (1992) Gene **114**, 139–143

Banaszak, L. J. and Bradshaw, R. A. (1975) Enzymes 3rd Ed. **11**, 369–396

Biellmann, J. F., Samama, J. P., Branden, C. I. and Eklund, H. (1993) Eur. J. Biochem. **102**, 107–110

Birktoft, J. J. and Banaszak, L. J. (1984) Peptide Protein Rev. **4**, 1–46

Birktoft, J. J., Rhodes, G. and Banaszak, L. J. (1989) Biochemistry **28**, 6065–6089
Bocanegra, J. A., Scrutton, N. S. and Perham, R. N. (1993) Biochemistry **32**, 2737–2740
Carter, P., Bedouelle, H. and Winter, G. (1985) Nucleic Acids Res. **13**, 4431–4443
Chambers, S. P., Prior, S. E., Barstow, D. A. and Minton, N. P. (1988) Gene **68**, 139–149
Chen, Z., Lee, W. R. and Chang, S. H. (1991) Eur. J. Biochem. **202**, 263–267
Clarke, A. R., Waldman, A. D., Hart, K. W. and Holbrook, J. J. (1985) Biochim. Biophys. Acta **829**, 397–407
Clermont, S., Corbier, C., Mely, Y., Gerard, D., Wonacott, A. and Branlant, G. (1993) Biochemistry **32**, 10178–10184
Cowan, D. A. (1992) Biochem. Soc. Symp. **58**, 149–169
Demchenko, A. P., Ruskyn, O. I. and Saburova, E. A. (1989) Biochim. Biophys. Acta **998**, 196–203
Feeney, R., Clarke, A. R. and Holbrook, J. J. (1990) Biochem. Biophys. Res. Commun. **166**, 667–672
Fersht, A. R., Jian-Ping, S., Knill-Jones, J., Lowe, D. M., Wilkinson, A. J., Blow, D. M., Brick, P., Carter, P., Waye, M. M. Y. and Winter, G. (1985) Nature (London) **314**, 235–238
Frieden, C. and Fernandez Sousa, J. (1975) J. Biol. Chem. **250**, 2106–2113
Gomi, T., Takata, Y., Date, T., Fujioka, M., Aksamit, R. R., Backlund, P. S., Jr. and Cantoni, G. L. (1990) J. Biol. Chem. **265**, 16102–16107
Gornall, A. G., Baradawill, C. J. and David, M. M. (1949) J. Biol. Chem. **177**, 751–766
Grimshaw, C. E., Matthews, D. A., Varughese, K. I., Skinner, M., Xuong, N. H., Bray, T., Hoch, J. and Whiteley, J. M. (1992) J. Biol. Chem. **267**, 15334–15339
Gutman, M. and Hartstein, E. (1977) Biochim. Biophys. Acta **481**, 33–41
Hall, M. D., Levitt, D. G. and Banaszak, L. J. (1992) J. Mol. Biol. **226**, 867–882
Hart, K. W. (1989) Ph.D. Thesis, University of Bristol
Hill, E., Tsernoglou, D., Webb, L. and Banaszak, L. J. (1972) J. Mol. Biol. **72**, 577–591
Hones, G., Hones, J. and Hauser, M. (1986a) Biol. Chem. Hoppe-Seyler **367**, 103–108
Hones, G., Hones, J. and Hauser, M. (1986b) Biol. Chem. Hoppe-Seyler **367**, 95–102
Hones, J. (1985) Biol. Chem. Hoppe-Seyler **366**, 561–566
Kelly, C. A., Nishiyama, M., Ohnishi, Y., Beppu, T. and Birktoft, J. J. (1993) Biochemistry **32**, 3913–3922
Lodola, A., Shore, J. D., Parker, D. M. and Holbrook, J. (1978) Biochem. J. **175**, 987–998
MacGregor, L. C. and Matschinsky, F. M. (1984) Anal. Biochem. **141**, 382–389
Mittl, P. R., Berry, A., Scrutton, N. S., Perham, R. N. and Schultz, G. E. (1993) J. Mol. Biol. **231**, 191–195
Nicholls, D. J., Sundaram, T. K., Atkinson, T. and Minton, N. P. (1990) FEMS Microbiol. Lett. **70**, 7–14
Nishiyama, M., Birktoft, J. J. and Beppu, T. (1993) J. Biol. Chem. **268**, 4656–4660
Oppenheimer, N. J., Arnold, L. J. and Kaplan, N. O. (1971) Proc. Natl. Acad. Sci. U.S.A. **68**, 3200–3205
Pace, C. N. (1986) Methods Enzymol. **131**, 266–280
Pace, C. N. (1990) Trends. Biotechnol. **8**, 93–98
Piontek, K., Chakrabarti, P., Schar, H.-P., Rossman, M. G. and Zuber, H. (1990) Proteins **7**, 74–92
Roderick, S. L. & Banaszak, L. J. (1986) J. Biol. Chem. **261**, 9461–9464
Sambrook, T., Fritsch, E. F. and Maniatis, T. (1989) in Molecular Cloning: a Laboratory Manual, Cold Spring Harbor Laboratory Press, Cold Spring Harbor, NY
Sanger, F., Nicklen, S. and Coulson, A. R. (1977) Proc. Natl. Acad. Sci. U.S.A. **74**, 5463–5467
Silverstein, E. and Sulebele, G. (1969) Biochim. Biophys. Acta **185**, 297–304
Smith, K., Sundaram, T. K., Kernick, M. and Wilkinson, A. E. (1982) Biochim. Biophys. Acta **708**, 17–25
Sundaram, T. K., Wright, I. P. and Wilkinson, A. E. (1980) Biochemistry **19**, 2017–2022
Telegdi, M., Wolfe, D. V. and Wolfe, R. G. (1973) J. Biol. Chem. **248**, 6484–6489
Waldman, A. D. B., Hart, K. W., Clarke, A. R., Wigley, D. B., Barstow, D. A., Atkinson, T., Chia, W. N. and Holbrook, J. J. (1988) Biochem. Biophys. Res. Commun. **150**, 752–759
Whitaker, J. R., Yates, D. W., Bennett, N. G., Holbrook, J. J. and Gutfreund, H. (1974) Biochem. J. **139**, 677–697
Wraight, C., Day, A., Hoogenraad, N. and Scopes, R. (1985) Anal. Biochem. **144**, 604–609

Received 7 June 1994/26 August 1994; accepted 2 September 1994